Nanoscale

Controlling Magic Size of White Light-emitting CdSe Quantum Dots

Journal:	*Nanoscale*
Manuscript ID	NR-ART-02-2018-001455.R1
Article Type:	Paper
Date Submitted by the Author:	10-Apr-2018

Complete List of Authors:	Dai, Sheng; University of California-Irvine, Chemical Engineering and Material Science Su, Yu-Sheng; National Formosa University, Department of Materials Science and Engineering Chung, Shu-Ru; National Formosa University, Department of Materials Science and Engineering Wang, Kuan-Wen; National Central University, Institute of Materials Science and Engineering Pan, Xiaoqing; University of California Irvine, Chemical Engineering and Materials Science

SCHOLARONE™
Manuscripts

Please do not adjust margins

Journal Name

ARTICLE

Controlling Magic Size of White Light-emitting CdSe Quantum Dots

Received 00th January 20xx,
Accepted 00th January 20xx

DOI: 10.1039/x0xx00000x

www.rsc.org/

Sheng Dai [a], Yu-Sheng Su [b], Shu-Ru Chung [b,*], Kuan-Wen Wang [a,c,*], and Xiaoqing Pan [a,d,*]

White light-emitting quantum dots (QDs) have shown brilliant prospects as white-light source in solid-state lighting devices, however, the commercial application is limited by their low fluorescence quantum yield (QY). Here, we report a facile thermal pyrolyzed organometallic route to synthesize white-light emitting CdSe QDs with enhanced QY, by employing particular non-coordinating solvent and long carbon chain amine. By clarifying the three distinct growing stages of CdSe nanocrystals, we are able to grasp critical growth parameters for high quality magic size QDs. According to the optical measurement and advanced characterization result, the as-synthesized magic-size QD samples show an enhanced QY (up to 64%) and an ultra high stability with no degradation even after 120 days, while the fabricated WLED devices also exhibit desirable properties (e.g., high QY and CRI, decent efficacy), demonstrating progress towards the desired efficiency of a commercially viable solid-state lighting device.

Introduction

White light-emitting quantum dots (QDs) have attracted significant research attention in the past decade since they show brilliant prospects as white-light source in efficient solid-state lighting devices [1-3]. The nanocrystals, smaller than 2 nm in diameter, exposing majority of their atoms on the surface, give rise to the characteristic emission from surface trap states and emit white light directly[4,5]. As opposite to a combination of different monochromatic QDs which together emit white light[6,7], white light-emitting QDs offer a solution to the drawbacks of current white light emitting diodes (WLEDs), such as a low color rendering index (CRI), self-absorption effect[8], and have been incorporated into prototypical frequency down converting devices[9,10].

However, the application of white light-emitting QDs is limited by their emission efficiency at the current stage, since the fluorescence quantum yield (QY) is usually below 27%[3,11-13], too low for the commercial use. Only if the efficiency would be greatly improved, can the white light-emitting QDs be used widely as a single source broad spectrum solid state lighting device. Based on this purpose, various methods have been developed to improve the performance of white light-emitting CdSe QDs through size control[14,15] and surface alternation[5,11,13,16-17], however, the optimized preparation process has not been achieved yet. From a fundamental standpoint, the growth mechanism of the white light-emitting QDs still remains elusive[18], raising the difficulties in grasping optimal synthesis conditions.

Here, we report a facile thermal pyrolyzed organometallic route to synthesize white-light emitting CdSe QDs, showing enhanced QY while still maintaining surface trap states, by employing particular non-coordinating solvent and long carbon chain amine. In this study, three distinct nucleation/growth stages are clarified of CdSe nanocrystals, enabling us to grasp critical parameters for high quality magic size QDs. According to the optical measurement and advanced characterization result, as-synthesized magic-size QD samples show an enhanced QY (up to 64%) and an ultra high stability with no degradation even after 120 days, while the fabricated WLED devices also exhibit desirable properties (*e.g.,* high QY and CRI, decent efficacy), demonstrating progress towards the outstanding performance of a commercially viable solid-state lighting device.

Experimental

Chemicals and Materials

Cadmium oxide (CdO, 99.999%, from Alfa Aesar), selenium powder (Se, 99.99%, Aldrich) hexadecylamine (HDA, 90%, Aldrich), oleic acid (OA, 90%, Aldrich), trioctylphosphine (TOP, 90%, Aldrich) and 1-octadecene (ODE, 90%, Aldrich) were used

[a] Department of Chemical Engineering and Materials Science, University of California-Irvine, Irvine, California 92697, United States
[b] Department of Materials Science and Engineering, National Formosa University, No.64, Wun Hua Road, Huwei Township, Yunlin County, 63201, Taiwan
[c] Institute of Materials Science and Engineering, National Central University, No. 300, Zhongda Rd., Zhongli District, Taoyuan City 32001, Taiwan
[d] Department of Physics and Astronomy, University of California-Irvine, Irvine, California 92697, United States
Corresponding Authors:
* (S.C.) E-mail: srchung@nfu.edu.tw
* (K.W.) E-mail: kuanwen.wang@gmail.com
* (X.P.) E-mail: xiaoqinp@uci.edu
Electronic Supplementary Information (ESI) available: [Detailed absorption and emission wavelengths of the as-synthesized CdSe QD samples, aged samples, devices properties of fabricated WLEDs. More detailed FL and UV-Vis spectra, XPS spectra, and CIE coordinates of the fabricated WLED devices.]

This journal is © The Royal Society of Chemistry 20xx

Please do not adjust margins

for the synthesis**.** Standard dye, rhodamine 101, used in quantum yield (QY) measurement was also provided by Aldrich.

Synthesis of White CdSe QDs

White light-emitting CdSe QDs were prepared by a thermal pyrolyzed organometallic route. The Cd-OA precursor was prepared by mixing 0.3 mmol of CdO and 0.8 ml of OA in a three-necked flask and then heated to 180 ^{o}C under Ar flow until a yellow transparent solution was obtained. Then, the solution was cooled down to room temperature (RT). In the next step, 6.0 mmol of ODE and HDA was added into the three-necked flask, stirred together under Ar flow at RT, and then the solution was reheated at various temperatures from 160-220 ^{o}C to prepare white CdSe QDs. 0.3 mmol of Se powder dissolved in 0.2 mL of TOP was injected into the three-neck flask under the given temperatures. Subsequently, a small amount of solution was taken out at desired reaction time and CdSe nuclei were formed quickly. After purification, the precipitate was dissolved and dispersed in hexane to remove unreacted reagents for further measurements.

Fabrication of WLED Devices

As-prepared CdSe QDs were used for white light diode (WLED) applications. WLED devices were fabricated by using 3020 surface-mounted device (SMD) typed InGaN/GaN-based near-UV and InGaN-based blue emitting LEDs with 13 mil. The QD samples and thermal cured epoxy gel (with different weight ratios) were packed as a convert type and cured at RT for 6 h to form WLED. The device performance was measured by integrating the sphere (Isuzu Optics, ISM-360) under a driving-current of 20 mA.

Characterization Techniques

Aberration-corrected scanning transmission electron microscopy (AC-STEM) was performed on a JEOL Grand ARM equipped with two spherical aberration correctors at 300 kV. High angle annular dark field (HAADF) images were recorded using a convergence semi angle of 22 mrad, and inner- and outer collection angles of 83 and 165 mrad, respectively.

Synchrotron-based X-ray diffraction (XRD) measurements were performed at Taiwan Beamline 12B2 at SPring-8. XRD data were collected at the wavelength of 0.68898 Å (18 keV), and then converted to the wavelength of 0.15418 Å by using the WinPLOTR software. XPS measurements were carried out on a Thermo VG Scientific Sigma Probe utilizing an Al Kα radiation to investigate surface compositions and chemical states of as-prepared GRx QDs.

Optical properties of the CdSe QDs were measured via a UV-vis spectrometer (UV-vis, Hitachi UH-5300 spectrometer) and a fluorescence spectrophotometer (FL, Hitachi F-7000). Relative QY of the synthesized samples were determined by comparing the area under the curve of FL emission for the CdSe QDs with that of fluorescent dye (rhodamine 101 in ethanol).

Results and discussion

In this study, precursor CdO with relatively low reactivity, instead of those highly reactive cadmium source like $Cd(CH_3)_2$, was used for the synthesis of white light-emitting QDs, undergoing a quick quenching at various temperatures between 160 ^{o}C and 220 ^{o}C. By using a combined reagents of non-coordinating solvent and long carbon chain amines (OA/ODE/HDA), the growth of CdSe QDs can be controlled precisely in a short time under relatively reaction temperatures, and was investigated systematically at the second time scale, which has never been done before. The morphology and structure information of the as-synthesized CdSe QDs was carefully characterized by aberration-corrected scanning transmission electron microscopy (AC-STEM), which provides an enhanced contrast of atomic-scale images of nanocrystals over a high background[19]. Here, Fig. 1a shows a low magnification HAADF-STEM image of the CdSe QDs synthesized at the temperature of 160 ^{o}C within 180 seconds. Clearly, ultra-small CdSe nanocrystals with homogeneous size are observed. Based on our STEM observation, the average size of these CdSe nanocrystals is measured to be 1.5 nm, less than 2.0 nm, corresponding to a minimum dimension of stable spherical nucleus defined as magic size (M)[3,20]. Particularly, Fig. 1b presents an atomic-scale HAADF image of a M-CdSe QD with its diameter of 1.8 nm, revealing its crystalline structural feature. According to the corresponding fast Fourier transform (FFT) pattern and the indexing result (Fig. 1c), the structure is determined to be zinc blende, which prefers to nucleate at this temperature[21].

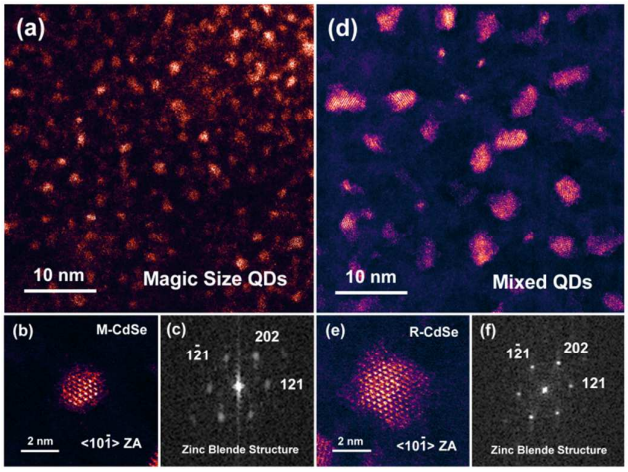

Figure 1. AC-STEM characterization of the as-prepared white light-emitting CdSe QDs. (a) Low magnification STEM image of the magic size (M) QDs synthesized at 160 ºC within 180 seconds. (b-c) Atomic-scale STEM image and corresponding FFT pattern showing the zinc blende structure of M-CdSe QDs. (d) Low magnification STEM image of the white light-emitting QDs prepared at 160 ºC after 600 seconds, containing magic size and regular size (R) QDs. (e-f) Atomic-scale STEM image and corresponding FFT pattern showing the zinc blende structure of R-CdSe QDs.

For comparison, Figs. 1d-1f present another batch of STEM images of the CdSe QDs grew at 160 ^{o}C for more than 600

This journal is © The Royal Society of Chemistry 20xx

seconds. This time, a mixed nanostructure, including not only nanocrystals of magic sizes, but also the QDs of regular sizes (R) larger than 2.0 nm, is observed. One of the typical HAADF-STEM images of R-CdSe QDs is shown in Figure 1e, while its zinc blende structure can also be identified through the indexing of the corresponding FFT pattern (Fig. 1f), consistent with the XRD results displayed in Figure S1 in the Supporting Information.

Furthermore, additional details of QD nucleation and growth were monitored within more different reaction time at the temperature of 160 °C. Here, Fig. 2 presents an evolution of FL emission and UV-vis absorption spectra from 60 seconds to 3600 seconds. At the beginning stage (60 s~300 s), M-CdSe QDs first started to nucleate because of a high monomer activity[22], showing a signature of M-QD formation evidenced by an emission peak at 440 nm, which is developing an absorption edge centered at 403 nm in the UV-Vis spectra[23]. At the meantime, a broad emission peak is observed around 540 nm (as marked by the blue arrows in Fig. 2b), while no corresponding absorption edge is found, indicating this is attributed to the deep trap emission[3,20]. The inset of Stage 1 in Fig. 2a shows a photograph of the QD solution upon UV excitation, collected at the reaction time of 180 seconds (more images of photoluminescence at each reaction stage can be found in the Supporting Information). Clearly, while color is exhibited in the M-QD solution, demonstrating that two critical factors, magic size and deep trap feature enable the while light emission.

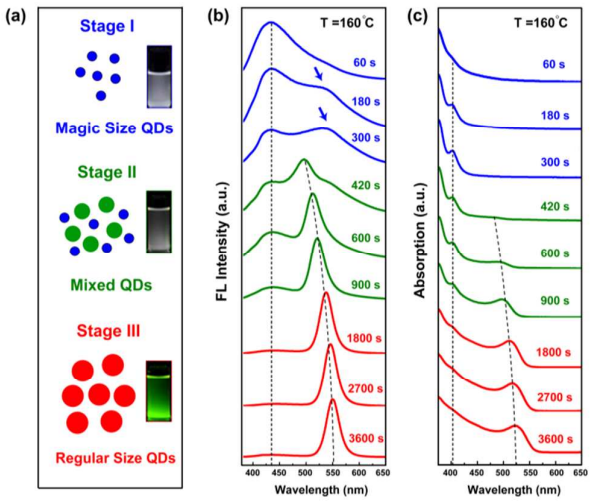

Figure 2. Schematics and corresponding spectra showing the three stages of CdSe QD growth. (a) Schematic diagrams showing three growing stages of the QDs under our synthesis condition. Insets are the corresponding photographs of vials containing CdSe QD solution. (b-c) FL emission and UV-Vis absorption spectra of CdSe QDs prepared at 160 ºC within different reaction time. Blue, green and red lines are corresponding to the three stages in (a).

Then in the next stage, as shown by the green spectra in Fig. 2, an additional set of emission/absorption peaks appear at longer wavelengths (around 500 nm/480 nm) after a reaction time of 420 s, suggesting a second round of nucleation taking place in the residual precursor. According to the peak position, the average diameter of the new born CdSe QDs is calculated to be larger than 2.5 nm, corresponding to the larger crystals, R-CdSe QDs, we observed in the STEM images (Figs. 1d and 1e). The nucleation of R-QDs is attributed to two reasons: (1) a less capping protection due to the consumption of surfactants during the first round of M-QD formation; (2) a depletion of the monomer concentration, making the dynamic critical size becoming larger. The R-QD peak position shifts to the longer wavelength region progressively, mirroring the continuous growth of the R-CdSe QDs. In contrast, the peak of M-QDs is fairly stable at the position of 440 nm while the intensity is unchanged in both emission and absorption spectra, suggesting the M-CdSe QDs only undergo a nucleation step without any further growth or ripening[17,24]. As shown in the green emission spectra, the peak intensities of M-QDs and R-QDs are still comparable, indicating the proportion between these two groups are similar during this stage. White light is still generated, as observed in the photograph of Stage 2, which was taken from the sample reacted for 600 seconds.

Moreover, prolonging the reaction time (> 1800 s) leads to further nucleation and growth of R-QDs, as shown in the red spectra, resulting in a remarkably stronger intensity and further red shift of the R-QD peak. Meanwhile, the intensity of the M-QD peak was decreasing from 82.0 to 37.0 during the elapsed time from 900 s to 1800 s (more quantitative results please see Fig. S2 in the Supporting Information). This trend is also observed in the next additional 900 seconds (1800 s~2700 s), indicating the gradual disappearance of the M-QDs at this stage, which is resulted from a dramatic decrease of the monomer activity due to the depletion of monomer concentration after the first two growing stages[25]. Thus, dominant population of the solution is becoming R-CdSe QDs, exhibiting a green color in the photograph.

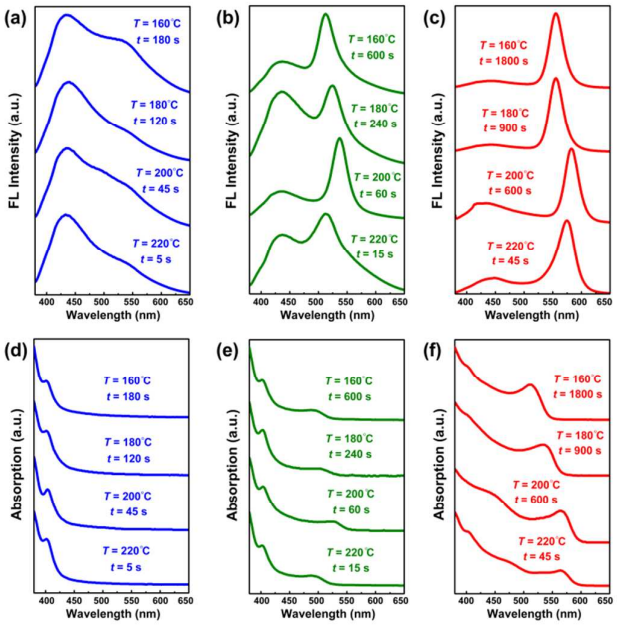

Figure 3. FL emission (a-c), and UV-Vis absorption (d-f) spectra of CdSe QDs growing at various temperatures within different reaction times. Blue, green, and red colors indicate the three growth stages illustrated in Figure 2a, respectively.

For a further systematic investigation of the growth dynamics, we synthesized CdSe QDs at more different temperatures (160, 180, 200, and 220 °C) within various reaction times down to the second scale. Under each temperature, the reaction time for the three stages are summarized in Fig. 3. According to the emission and absorption spectra in Figs. 3a and 3d, the nucleation time of M-CdSe QDs changes dramatically from 180 s to 5 s while the temperature is elevated form 160 °C to 220 °C, reflecting a strong dependence of the supersaturation and nucleation energy barrier on the reaction temperature (More details of the nucleation and growth evolution at the temperature of 180 °C, 200 °C and 220 °C can be found in Figs. S3-S5). In addition, the evolution time from M-QDs (Stage I, blue spectra) to R-QDs (Stage III, red spectra) is decreasing from 1800 s to only 45 s as the temperature increasing from 160 °C to 220 °C. The accelerated growth rate of R-QDs at higher temperatures is in accordance with the kinetic rule of nanocrystal growth[25]. Furthermore, a controlled synthesis experiment is performed under 160 °C, and the dosage of the capping reagents (*e.g.*, HDA and ODE) was reduced to half intentionally. As a result (see Fig. S6 in the Supporting Information), the evolution time from the beginning to Stage II, is reduced from 420 s to 120 s, compared to the previous result in Fig. 2. Thus the effect of capping reagents is disclosed: more capping reagents are able to slow down the nucleation and growth of R-QDs. In another word, based on the above results, lower temperatures and higher dosage of capping reagents are both favourable for the control and synthesis of M-QDs.

	M-QDs	Mixed QDs	R-QDs
160 °C	58%	40%	3%
180 °C	42%	37%	8%
200 °C	48%	39%	8%
220 °C	64%	45%	6%
180 °C-A	47%	42%	6%

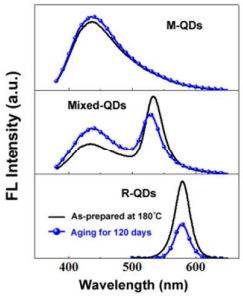

Figure 4. QY of M-QDs, Mixed-QDs, and R-QDs synthesized under various reaction temperatures (left panel). 180 °C-A is noted for the sample synthesized at 180 oC and then aged for 120 days, whose FL emission spectra is presented in the right panel.

Figure 4 shows the corresponding quantum yield (QY) of all the 12 kinds of CdSe samples in Fig. 3. Noticeably, the M-QD samples we synthesized are always endowed with desirable QYs in a range of 42%~64%, much higher than those M-QDs reported in published literatures[3, 11-13]. Besides, it is revealed that the QY decreases in M-QDs, mixed-QDs, and R-QDs groups in sequence under each temperature, showing a deteriorating QY as an increase of the fraction of R-QDs. Actually, this is a result of the different surface chemical states of M- and R-QDs, which is demonstrated by our X-ray photoelectron spectroscopy (XPS) characterization. For example, Fig. S7 presents a comparison of XPS spectra of the sample acquired at the three growing stages under 180 °C, revealing that Cd is always retaining its metallic state in all the samples. However, in contrast, metallic Se is only observed in M-QD samples while obvious SeO_x phase is revealed in the mixed-QD and R-QD groups. R-QDs growing at late stages are easier to be oxidized due to a less protection from surfactants, as discussed above, and thus deteriorates their QY[26].

In addition, a 120-day aging test was further performed on the samples synthesized at 180 °C (noted as 180 °C-A), and the QY and emission spectra after the aging test are also presented in Fig. 4 (detail results are summarized in Table S2). It is interesting to find the intensity of the M-QD peak was enhanced in both M-QDs and mixed-QDs after 120 days, resulting in promoted QY of the two samples. Such desirable stability and improved emission properties are attributed to the surface reconstruction[27] occurring at the well-protected CdSe surface without oxidation. The driving force of the surface reconstruction process is from the surface tension. The smaller the QDs are, the stronger the surface tension will drive the surface reconstruction process and, thus, to minimize the nonradiative traps originated from the dangling bonds on the surface of the QDs[28]. However, for the R-QD peak in the mixed-QDs and R-QDs groups, the intensities continued to decline during the aging test, corresponding to a loose protection and a desorption of the surfactants.

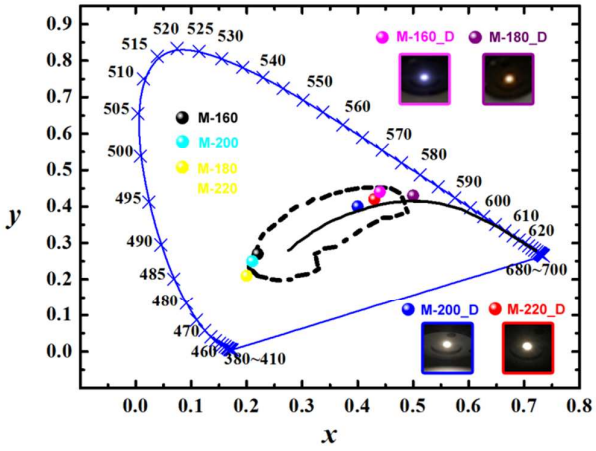

Figure 5. CIE coordinates of M-CdSe QDs prepared at various temperatures and corresponding WLED devices (noted as D). Insets are optical images showing the exhibiting light of the M-QD-based WLED devices.

The above results and discussion help us to understand and grasp the critical parameters for the growth of M-QDs, thus producing high quality white light-emitting CdSe QDs for the device application. WLED devices are fabricated based on the four M-QD samples synthesized at various temperatures

This journal is © The Royal Society of Chemistry 20xx

(noted as M-160_D for example). Since the QD samples have to be purified during the device fabrication, in which the surfactants are removed and the concentrations of QDs are increased, CIE coordinates of the WLED devices are moving towards the white light region, compared to those of the as-synthesized M-QDs (Fig. S8), as shown in Fig. 5. Although the device properties are inevitably changed by the fabrication procedures: *e.g.*, QYs are influenced by the purification; devices efficacies are affected by the power of UV chips, the obtained WLEDs still inherit the excellent properties of our M-QD samples, showing desirable device properties: 31%~39% of QYs, and 0.7~2.0 lm/W of efficacies (more details please see Table S3 in the supporting information), demonstrating a great enhancement compared to the previous result in literature[3]. In addition, it is worth mentioning that color rendering index (CRI) of all the devices are higher than 80, while the correlated color temperature (CCT) values are all located within the ideal region[29] for white-light LEDs, considered to be more than acceptable for most display and lighting applications.

Conclusions

In summary, we here report a facile thermal pyrolyzed organometallic route to synthesize high quality white-light emitting CdSe QDs at relatively low temperatures, by employing particular non-coordinating solvent and long carbon chain amine. Based on our systematic investigation on the nucleation and growth evolution, we clarified the three distinct growing stages of CdSe nanocrystals, and are able to grasp critical parameters to obtain high quality magic size QDs. According to the optical measurement and advanced characterization result, the as-synthesized magic-size QDs show an enhanced QY (up to 64%) and an ultra high stability with no degradation even after 120 days. In addition, the fabricated WLED devices based on our M-QD samples, also present desirable properties, such as a high CRI, improved efficacy, and ideal CCT values. The findings in this study not only show important implications for the synthesis and control of white light-emitting QDs, but also demonstrate progress towards the desired efficiency of a commercially viable solid-state lighting device.

Conflicts of interest

The authors declare no competing financial interest.

Acknowledgements

This work was supported by the National Science Foundation (grant number DMR-1506535) and Ministry of Science and Technology of Taiwan (MOST 104-2628-E-008-005-MY3, 105-2221-E-150-058 and 106-2221-E-150-049). Additional support was provided by Irvine Materials Research Institute (IMRI).

Notes and references

1 S. Tonzani, *Nature* 2009, **459**, 312.
2 H. S. Chen, K. W. Wang, S. S. Chen, and S. R. Chung, *Optics Lett.* 2013, **38**, 2080.
3 M. J. Bowers II; J. R. McBride, S. J. Rosenthal, *J. Am. Chem. Soc.* 2005, **127**, 15378.
4 J. R. McBride, A. D. Dukes III, M. A. Schreuder, S. J. Rosenthal, *Chem. Phys. Lett.* 2010, **498**, 1.
5 T. E. Rosson, S. M. Claiborne, J. R. McBride, B. S. Stratton, S. J. Rosenthal, *J. Am. Chem. Soc.* 2012, **134**, 8006.
6 X. Xu, Y. Wang, T. Gule, *Mater. Res. Bull.* 2013, **48**, 983.
7 S. Nizamoglu, T. Ozel, E. Sari, *Nanotechnology* 2007, **18**, 065709.
8 H. Y. Lin, S. W. Wang, C. C. Lin, *IEEE J. Sel. Top. Quant. Electron* 2016, **22**, 2000107.
9 M. A. Schreuder, J. D. Gosnell, N. J. Smith, M. R. Warnement, S. M. Weiss, S. J. Rosenthal, *J. Mater. Chem.* 2008, **18**, 970.
10 M. A. Schreuder, K. Xiao,I. N. Ivanov, S. M. Weiss, S. J. Rosenthal, *Nano Lett.* 2010, **10**, 573.
11 X. Liu, Y. Jiang, C. Wang, S. Li, X. Lan, Y. Chen, *Phys. Status Solidi A* 2010, **207**, 2472.
12 B. M.Cossairt, J. S. Owen, *Chem. Mater.* 2011, **23**, 3114.
13 S. Dolai, P. Dutta, E. Sardar, *Chem. Mater.* 2015, **27**, 1057.
14 A. Kasuya, R. Sivamohan, Y. A. Barnakov, I. M. Dmitruk, T. Nirasawa, V. R. Romanyuk, V. Kumar, S. V. Mamykin, K. Tohji, B. Jeyadevan, K. Shinoda, T. Kudo, O. Terasaki, Z. Liu, R. V. Belosludov, V. Sundararajan, Y. Kawazoe, *Nat. Mater.* 2004, **3**, 99.
15 Y. Wang, Y. Liu, Y. Zhang, F. Wang, P. J. Kowalski, H. W. Rohrs, R. A. Loomis, M. L. Gross, W. E. Buhro, *Angew. Chem. Int. Ed.* 2012, **51**, 6154.
16 S. Dolai, P. R. Nimmala, M. Mandal, B. B. Muhoberac, K. Dria, A. Dass, R. Sardar, *Chem. Mater.* 2014, **26**, 1278.
17 S. Kudera, M. Zanella, C. Giannini, A. Rizzo, Y. Li, G. Gigli, R. Cingolani, G. Ciccarella, W. Spahl, W. J. Parak, L. Manna, *Adv. Mater.* 2007, **19**, 548.
18 S. M. Harrell, J. R. McBride, S. J. Rosenthal, *Chem. Mater.* 2013, **25**, 1199.
19 T. J. Pennycook, J. R. McBride, S. J. Rosenthal, S. J. Pennycook, S. T. Pantelides, *Nano Lett.* 2012, **12**, 3038.
20 A. D. Dukes III, M. A. Schreuder, J. A. Sammons, J. R. McBride, J. N. Smith, S. J. Rosenthal, *J. Chem. Phys.* 2008, **129**, 121102.
21 Z. Deng, L. Cao, F. Tang, B. Zou, *J. Phys. Chem. B* 2005, **109**, 16671.
22 W. W. Yu, Y. A. Wang, X. G. Peng, *Chem. Mater.* 2003, **15**, 4300.
23 L. Qu, W. W. Yu, X. G. Peng, *Nano Lett.* 2004, **4**, 465.
24 K. Yu, M. Z. Hu, R. Wang, M. L. Piolet, M. Frotey, M. B. Zaman, X. Wu, D. M. Leek, Y. Tao, D. Wilkinson, C. Li, *J. Phys. Chem. C* 2010, **114**, 3329.
25 Q. Dai, D. Li, J. Chang, Y. Song, S. Kan, H. Chen, B. Zou, W. Xu, S. Xu, B. Liu, G. Zou, *Nanotechnology* 2007, **18**, 405603.
26 X. Wang, L. Qu, J. Zhang, X. Peng, M. Xiao, *Nano Lett.* 2003, **3**, 1103.
27 A. Puzder, A. J. Williamson, F. Gygi, G. Galli, *Phys. Rev. Lett.* 2004, **92**, 217401-1.
28 J. Y. Zhang, X. Y. Wang, M. Xiao, L. Qu, X. Peng, *Appl. Phys. Lett.* 2002, **81**, 2076.
29 B. W. D'Andrade, S. R. Forrest, *Adv. Mater.* 2004, **16**, 1585.